SYNTHESIS AND PHOTOCATALYTIC ACTIVITY OF C, N AND S DOPED TiO_2 UNDER VISIBLE LIGHT

Đến tòa soạn 02-06-2022

Nguyen Thi Lan[1*], Nguyen Phi Hung[2]
[1]*Faculty of Natural Sciences, Quy Nhon University*
[2]*QNU Institute of Educational Sciences (QNIES)*
*Email: nguyenthilan@qnu.edu.vn

TÓM TẮT

TỔNG HỢP VÀ HOẠT TÍNH QUANG XÚC TÁC CỦA TiO_2 PHA TẠP C, N VÀ S DƯỚI VÙNG ÁNH SÁNG KHẢ KIẾN

Vật liệu TiO_2 pha tạp các nguyên tố phi kim C, N và S được tổng hợp bằng phương pháp thủy nhiệt từ dung dịch titanyl sulfate với các tiền chất pha tạp khác. Sự ảnh hưởng của các nguyên tố pha tạp vào cấu trúc tinh thể, hình thái học, diện tích bề mặt, trạng thái liên kết và khả năng hấp thụ ánh sáng được đặc trưng qua các phương pháp XRD, UV-Vis-DRS và XPS. Sự hình thành các liên kết mới Ti-O-C, O-N-Ti, sự chèn các nguyên tố phi kim vào mạng tinh thể TiO_2 hay sự thay thế ion Ti^{4+} bằng S^{6+} đã tạo ra sự chuyển dịch đỏ năng lượng vùng cấm của vật liệu pha tạp. Kết quả chứng minh rằng, vật liệu TiO_2 đồng pha tạp cả ba nguyên tố C, N và S (TH-TiO_2) cho hoạt tính quang xúc tác tốt nhất qua sự phân hủy chất kháng sinh tetracycline trong dung dịch nước dưới vùng ánh sáng nhìn thấy. Sự tăng hoạt tính quang xúc tác của vật liệu đồng pha tạp TH-TiO_2 so với các thành phần pha tạp nguyên tố riêng lẻ là do sự giảm tốc độ tái tổ hợp của các cặp electron-lỗ trống quang sinh.

***Từ khóa**: Tổng hợp, chất xúc tác quang, TiO_2, pha tạp, tetracycline*

1.INTRODUCTION

Population growth has increased the demand for food production, which has led to aquaculture becoming an important agricultural industry worldwide. With the advantage of being a country with a sea area of 3,448,000 km^2 and a coastline of 3260 km, Vietnam has favorable conditions to develop the aquaculture, fishing, and seafood processing industry. Therefore, in recent years, the shrimp farming industry has grown in size and number of farming establishments to meet the needs of domestic and foreign markets. Parallel with the industry's rise are the environmental consequences, especially the large amount of wastewater from shrimp ponds that discharge much untreated polluted sewage. Several chemical and biological compounds have been mainly used in aquaculture production worldwide. Compounds that carry many environmental risks, such as antibiotics, pesticides, and disinfectants, are highly toxic and are among the most dangerous pollutants. In the long term, the discharge of aquatic animals into water bodies contributes to environmental pollution and directly impacts marine communities of water receptors, thereby reducing water quality [1]. Excretion and food waste accumulate during shrimp culture, often decreasing water quality and negatively affecting shrimp growth and the environment. Shrimp farming wastewater contains significant amounts of nitrogen, phosphorus, organic matter, and

xenobiotics such as antibiotics and hormones, which can damage the habitat of natural aquatic species, causing a decrease in oxygen levels in the water. Pollutants are treated by standard absorption, sedimentation, filtration, membrane [2], and biological treatment. Although treatment costs are high and may produce harmful secondary pollutants, these methods do not entirely remove persistent organic compounds in water, especially fats (which are difficult to decompose) destroyed by microorganisms. Countries are currently researching a promising and effective solution in water treatment to solve this problem, which is enhanced oxidation processes (AOPs).

Recently, different types of pollutants from industrial activities, agriculture, sewage, etc., are directly rejected to water bodies, causing water pollution. Therefore, removing pollutants from wastewaters is one of the major issues in the contemporary world [3].

AOPs include many different methods and directions [4], such as treatment with O_3, H_2O_2; Fenton process; TiO_2 photocatalysis is an open and potential development direction. After first being applied in water treatment in 1972-1977 [5, 6], there have been many studies related to this field. TiO_2 semiconductors can catalyze the oxidation of organic molecules that are difficult to decompose into smaller molecules. Titanium dioxide (TiO_2) is the most widely used photocatalyst for the decomposition of various organic pollutants because of its cheapness and nontoxicity, in addition to its high activity, optical properties, and chemical stability. The band gap energy of TiO_2 (3.0-3.2 eV) requires UV light irradiation, and thus only a small portion of the solar spectrum is absorbed in the UV region ($\lambda < 380$ nm) [7].

However, despite its many advantages, TiO_2 can only work under a narrow range of ultraviolet light [2]. According to the works [8] the modification of TiO_2 can increase the catalytic activity and expand the active light region to the visible area. Many studies have suggested that TiO_2 doped with nonmetal elements such as C, S and N can extend the absorption spectrum to the visible light region [9-11]. Inheriting those results, in this work, TiO_2 was prepared from ilmenite ore by using sulfuric acid method, and then TiO_2 modified C, N, and S was synthesized, investigated the activity, and it was used to study the photodegradation of tetracycline antibiotics in water solution under visible light and sunlight.

2. EXPERIMENTAL

2.1. Materials and synthesis

TiO_2 is prepared from Binh Dinh Ilmenite ore, Sulfuric acid (H_2SO_4, 98%), thiourea (CH_4N_2S, 99%), ammonium hydroxide (NH_4OH), glucose ($C_6H_{12}O_6$), sulfur (S), ethanol (C_2H_5OH), were purchased from Factory Co., Ltd (China), tetracycline hydrochloride ($C_{22}H_{24}O_8N_2.HCl$, 96.09%), was obtained from Drug Testing Institute in Ho Chi Minh City (Vietnam).

Synthesis of $TiOSO_4$ material from Binh Dinh ilmenite ore.

The sulfuric acid solution into a 500 mL heat-resistant flask and slowly add 50 g of ilmenite ore. The ore is decomposed for 1 hour (with stirring) at 200-210 ^oC on a stove away from the sand. The mixture after decomposition was allowed to cool naturally and then dissolved with H_2SO_4 0.005M solution on a heated magnetic stirrer for about 3 hours at 70 ^oC. Allow the mixture to settle for about 8 hours, then separate the liquid and solid residues. The filtrate after separation of solid residues is de-ferrous by using iron planers to reduce Fe^{3+} to Fe^{2+} [12, 13]. The solution after iron reduction is concentrated until scum. Continue to cool the solution after concentration at about -2 ^oC to -5 ^oC for 8 hours. After that, cold filtration was carried out to separate the iron in the form of $FeSO_4.7H_2O$, obtaining $TiOSO_4$ solution.

Synthesis of C, N, and S doped TiO_2 materials

Take 2.27 grams of $TiOSO_4$ synthesized from Ilmenite ore and a determined amount of thiourea (with the molar ratio of thiourea /TiO_2 = 2:1) were put in a Teflon flask dissolved with distilled water. Put the Teflon flask in the autoclave, and perform 180 ^oC hydrothermal for 12 hours.

After hydrothermal, the autoclave was allowed to cool naturally to room temperature. Filter the resulting white precipitate and wash it several times with distilled water until the filtrate has a constant pH. The obtained product was dried and calcined at 500 ^oC for 1 hour to get TH-TiO_2 material.

The synthetic single-element doping samples are similar to TH-TiO_2 materials. However, they replace thiourea with NH_4OH, glucose, and sulfur solutions in ethanol too, in turn, introduce nitrogen into the crystal structure of TiO_2 (N- TiO_2), C-doped TiO_2 material (C-TiO_2), sulfur-doped material (S-TiO_2). The mass of the doping agents was calculated based on the number of moles of each doping element in the TH-TiO_2 sample.

2.2. Photocatalytic activity

The catalytic activity of C-TiO_2, N-TiO_2, S-TiO_2, and TH-TiO_2 were estimated through the decomposition of tetracycline (10 mg/L) and the catalytic mass (0.6 g/L). The mixture was stirred in the dark for 30 minutes to reach the adsorption/desorption equilibrium, then illuminated with a 60W filament lamp (filter cut-off λ <400 nm), lighting distance of the lamp is 10 cm. The remaining tetracycline concentration was determined by the HPLC-UV method on Thermo Scientific series 3300 HPLC (Thermo Scientific Technologies, CA, USA) (λ_{max} = 355 nm).

2.3. Methods of analysis

The X-ray diffraction (XRD) was conducted in D8 - Advance 5005 with Cu Kα λ = 0.154 nm. The element composition and oxidation state on the catalyst surface in the sample was determined by X-ray electron spectroscopy (XPS) (ESCALab 250-Thermo VG, UK, Ewha Woman's University, Korea). The elemental analyses were conducted using EDX spectroscopy on JSM Jeol 5410LV (Japan).

3. RESULTS AND DISCUSSION

3.1. Characterization of materials

The composition of the material samples C-TiO_2, N–TiO_2, S–TiO_2, and TH-TiO_2 was investigated by an XRD diagram; the results are presented in Figure 1.

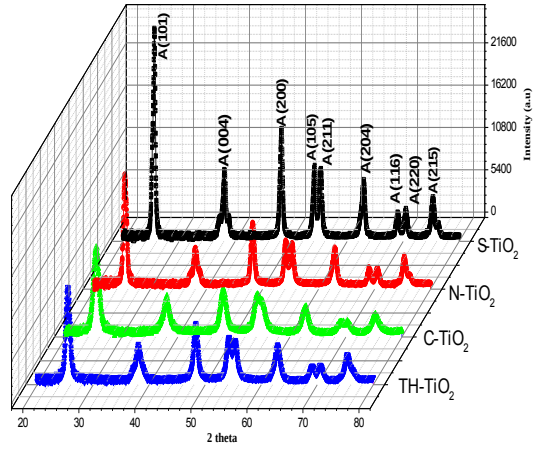

Figure 1. XRD patterns of C, N, and S modified TiO_2 samples.

From the figure, the peaks appear at 2θ = 25.3^o; 37.8^o; 48.1^o; 53.9^o; 55.0^o; 62.6^o; 68.8^o; 70.3^o; 75.1^o corresponds to the lattice faces (101), (004), (200), (105), (211), (204), (116), (220), (215) of the TiO_2 anatase phase [14]. Thus, it can be seen that the use of different doping agents does not affect the crystal structure of the material.

The oxidation states of C, N, and S in TH-TiO_2 were studied by XPS spectra (Figure 2).

XPS spectrum Figure 2a shows the N1s characteristic peaks of TH-TiO_2 and N-TiO_2 samples. According to [15], peaks with energy at 399.6 eV in N-TiO_2 and all peaks with energy ~400.0 eV appear due to the insertion of N atom into TiO_2 lattice or/and ON bond formation - Ti. Also, according to the author, N doping will form NO bonds and create a localized intermediate energy state (mid-gap high-localized states) which helps to raise the valence band energy and thus contribute to reducing the bandgap energy of the doped material. On the other hand, according to [16], the N1s peak of TH-TiO_2 (400.1 eV) is lower than the corresponding energy peak in the N-TiO_2 sample (400.7 eV) due to the presence of other elements, namely carbon and sulfur. This proves that C, N, and S elements have been successfully doped into TiO_2 crystal lattice.

XPS spectrum Figure 2b shows that all doped material samples have the appearance of peak

energy at 284.0 – 285.6eV. This energy value is defined as that of the control carbon (C1s) used in the measurement and is referred to as the adventitious carbon (AdC) [17]. The XPS spectrum of C in the TH-TiO_2 sample appeared to have characteristic peaks at 286.4 and 289.1 eV. According to [16], these two energy peaks are distinct from C-O and C=O bonds. According to [18], the formation of Ti-O-C carbonate groups is responsible for the appearance of the bond at 286.4 eV. Many studies show that the construction of carbonate groups incorporated into the interstitial positions of TiO_2 lattice helps reduce the material's bandgap energy and increase the absorption capacity of—the visible light [18]. The decrease in the binding energy of C1s in the TH-TiO_2 sample compared with the C-TiO_2 model is also attributed to the presence of N and S elements in the TiO_2 crystal lattice.

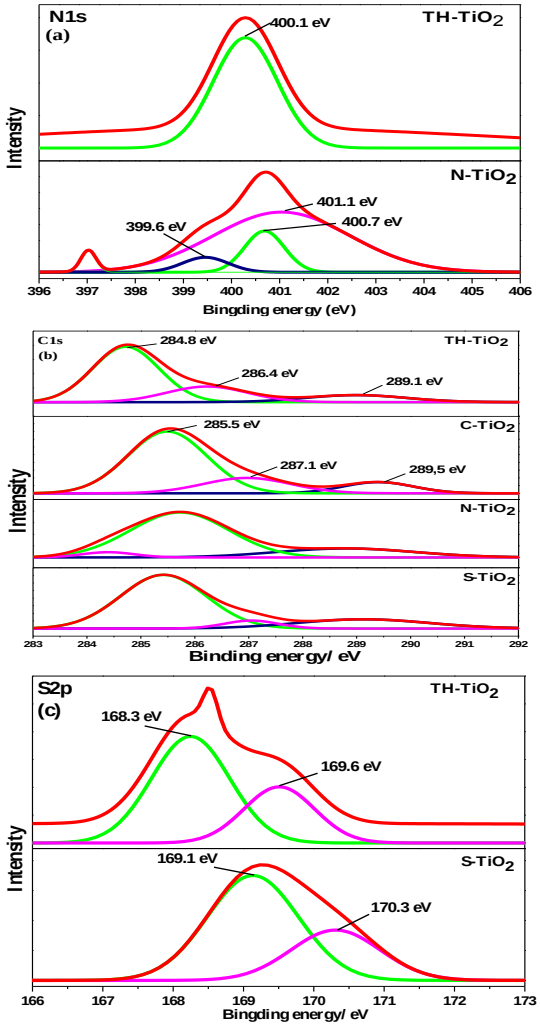

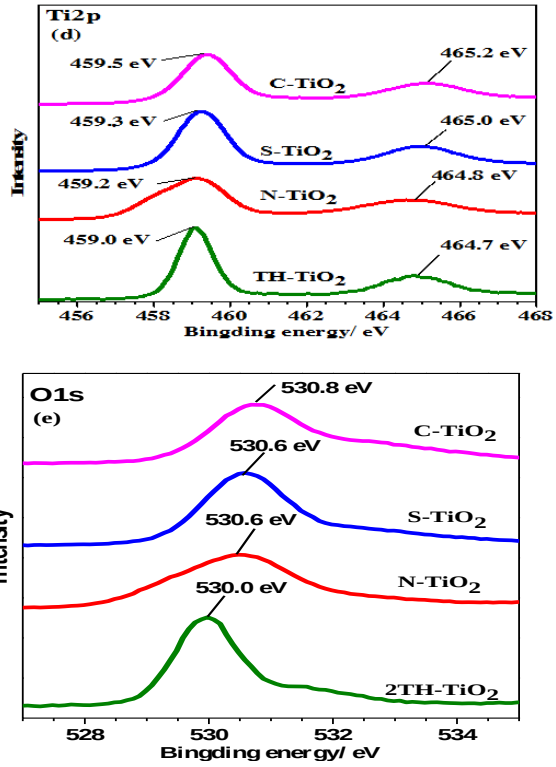

Figure 2. XPS spectrum of (a) N1s; (b) C1s; (c) S2p; (d) Ti2p; (e) O1s in samples TH-TiO_2, N-TiO_2; C-TiO_2; S-TiO_2.

The XPS S2p spectrum of TH-TiO_2 in Figure 2c peaks at 168.7 and 169.6 eV attributed to the S^{6+} group corresponding to the S^{6+} cation in the S=O SO bond formed when some Ti^{4+} ions in the TiO_2 lattice are replaced by sulfur atoms [19]. The peaks corresponding to Ti-S bonds were not found around the 160-163 eV positions because sulfur anion doping to form Ti-S bonds is often challenging. The S^{2-} ion (1.7 Å) has a much larger radius than the O^{2-} ion (1.22 Å), so significant energy is required to form Ti-S bonds instead of Ti- bonds. O. Therefore, the replacement of Ti^{4+} by S^{6+} is more favorable than O^{2-} by S^{2-}. This result was also verified by Ohno et al. when doping sulfur into TiO_2. Besides, Ohno also showed a charge imbalance created when the S^{6+} ion replaces the Ti^{4+} ion in the crystal lattice. The excess positive charge is neutralized by the hydroxyl ion, which increases the photocatalytic activity of the material [20]. Furthermore, according to [21], the doping of sulfur into TiO_2 forms a new energy structure,

which contributes to the reduction of the bandgap energy of the material. The XPS S2p spectrum of S-TiO_2 with peaks at 169.1 eV and 170.3 eV also characterizes the doped S^{6+} cation in TiO_2. However, the increase in the binding energy in the XPS spectrum from the TH-TiO_2 to the S-TiO_2 sample because the sulfur doping into the TH-TiO_2 selection requires higher formation energy than the single doping of the sulfur element into the TiO_2 [19].

XPS Ti2p spectrum of C, N, S-doped TiO_2 is shown in Figure 2d XPS Ti2p spectrum in TH-TiO_2 appears two primary components of Ti^{4+} state in TiO_2 are Ti2p3/2 and Ti2p1/2 at 459.0 and 464.7 eV [22]. The decrease in the binding energy of Ti2p from the C-TiO_2 sample to the TH-TiO_2 sample is caused by the electron interactions between Ti with anions and the formation of new bonds, causing partial electron transformations leading to an increase in the electron density on Ti. This confirms that C, N, and S elements have been successfully doped into TiO_2 [16].

The XPS O1s spectrum of the samples is shown in Figure 2e. The XPS of O1s of TH-TiO_2 appeared at a peak with the energy level of 530.0 eV, which is characteristic of O in the Ti-O bond in the TiO_2 lattice [23]. According to [24], after doping, elements C, N, and S will replace in place of O. A part of electrons from C, N, and S will move to Ti and further to O because element O has ample electronegativity electricity. As explained above, the increase in electron density on Ti and O is responsible for the decrease in the binding energy.

Figure 3 shows that N-TiO_2 and S-TiO_2 materials only absorb photons of ultraviolet light (below 400 nm). Meanwhile, the material samples TH-TiO_2 and C-TiO_2 can absorb photons of visible light.

The bandgap energy determined by the Kubelka–Munk function for samples TH-TiO_2, N-TiO_2, S-TiO_2, and C-TiO_2 is 2.88, 3.05, 3.15, and 2.70 eV, respectively.

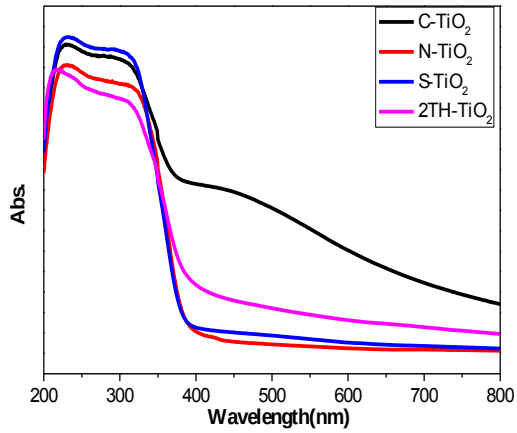

Figure 3. UV-Vis DRS spectra of TH-TiO_2, S-TiO_2, N-TiO_2, and C-TiO_2.

3.2. Catalytic activity

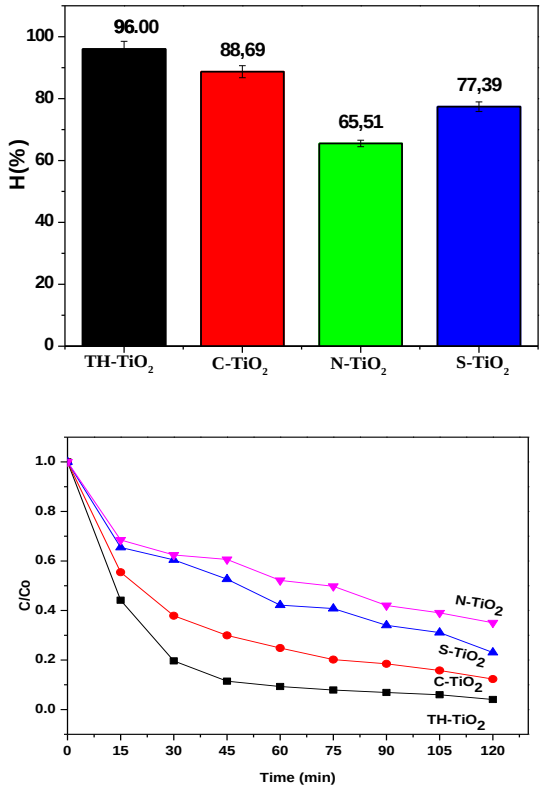

Figure 4. Photosynthetic efficiency of tetracycline degradation with different catalysts (conditions: mcatalyst = 0:6g·L^{-1}; concentration of TC = 10 mg.L^{-1}; adsorption time = 30 min)

From Figure 4, it is shown that TH-TiO_2 material exhibits the best photocatalytic activity with TC decomposition efficiency above 96%. The two samples, N-TiO_2 and S-TiO_2, performed relatively poorly in the visible light region.

Although the surface area is more extensive and the bandgap energy is smaller than that of S-TiO_2, the photocatalytic activity of N-TiO_2 is worse than that of S-TiO_2, which contradicts the above hypotheses. The test results of the isoelectric point of N-TiO_2 materials have clarified the above contradiction. N-TiO_2 materials are synthesized in an NH_4OH environment with pHpzc = 8. In a primary setting, the following equilibria occur, increasing the negatively charged centers on the material's surface [25], then there is the appearance of N-TiO_2 materials. There is a repulsive interaction between the anionic form of tetracycline and the negatively charged material surface, reducing the adsorption capacity of tetracycline, thereby reducing the tetracycline treatment efficiency.

$$-Ti-O-H+OH^- \rightarrow -Ti-O^- + H_2O$$

$$-Ti-N-H_2+OH^- \rightarrow -Ti-NH^- + H_2O$$

The results from Figure 4, it is shown that TH-TiO_2 material exhibits the best photocatalytic activity with TC decomposition efficiency above 96%. The two samples, N-TiO_2 and S-TiO_2, performed relatively poorly in the visible light region.

4. Conclusion

The modified TiO_2 materials samples C-TiO_2, N-TiO_2, S-TiO_2, and TH-TiO_2 were successfully prepared by hydrothermal method to reach nanometer particle size, low bandgap energy, and increased activity. In particular, the TH-TiO_2 material sample has the best photocatalytic activity on degradation of tetracycline, with degradation efficiency up to 96% after 120 minutes illumination under the visible light from (60W-220V) lamp. Photocatalytic activities of the TH-TiO_2 were markly improved due to the reducing of band gap energy and the less recombination of photo-generated electrons and holes.

References

[1] Silapajarn O. and Boyd C. E., (2005). Effects of channel catfish farming on water quality and flow in an Alabama Stream (in E). *Reviews in Fisheries Science,* **13(2)**, 109-140.

[2] Chong M. N., B. Jin, C. W. Chow, and C. Saint, (2010). Recent developments in photocatalytic water treatment technology: a review (in E). *Water research,* **44(10)**, 2997-3027.

[3] L. Dapeng and Q. Jiuhui, (2009). The progress of catalytic technologies in water purification: A review. *Journal of Environmental Sciences,* **21(6)**, 713-719.

[4] A. R. Ribeiro, O. C. Nunes, M. F. Pereira, and A. M. Silva, (2015). An overview on the advanced oxidation processes applied for the treatment of water pollutants defined in the recently launched Directive 2013/39/EU. *Environment international,* **75**, 33-51.

[5] A. Fujishima and K. Honda, (1972). Electrochemical Photolysis of Water at a Semiconductor Electrode (in E). *Nature,* **238(5358**), 37–38.

[6] Frank S. N. and Bard A. J., (1977). Heterogeneous photocatalytic oxidation of cyanide and sulfite in aqueous solutions at semiconductor powders, (in E). *The Journal of Physical Chemistry,* **81(15)**, 1484-1488.

[7] D. Chen, Z. Jiang, J. Geng, Q. Wang, and D. Yang, (2007). Carbon and nitrogen co-doped TiO_2 with enhanced visible-light photocatalytic activity. *Industrial & engineering chemistry research,* **46(9)**, 2741-2746.

[8] Li Hexing, Li Jingxia, and Huo Yuning, (2006). Highly active TiO_2N photocatalysts prepared by treating TiO_2 precursors in NH_3/ethanol fluid under supercritical conditions (in E). *The Journal of Physical Chemistry B,* **110(4),** 1559-1565.

[9] P. Periyat, S. C. Pillai, D. E. McCormack, J. Colreavy, and S. J. Hinder, (2008). Improved high-temperature stability and sun-light-driven photocatalytic activity of sulfur-doped anatase TiO_2. *The Journal of Physical Chemistry C,* **112(20)**, 7644-7652.

[10] M.-S. Wong, S.-W. Hsu, K. K. Rao, and C. P. Kumar, (2008). Influence of crystallinity and carbon content on visible light photocatalysis of carbon doped titania thin films. *Journal of*

Molecular Catalysis A: Chemical, **279(1)**, 20-26.

[11] I.-C. Kang, Q. Zhang, S. Yin, T. Sato, and F. Saito, (2008). Novel method for preparation of high visible active N-doped TiO_2 photocatalyst with its grinding in solvent. *Applied Catalysis B: Environmental,* **84(3-4)**, 570-576.

[12] Z. Li, Z. Wang, and G. Li, (2016). Preparation of nano-titanium dioxide from ilmenite using sulfuric acid-decomposition by liquid phase method. *Powder Technology,* **287**, 256-263.

[13] Nguyễn Mạnh Tiến, Ngô Sỹ Lương, Nguyễn Văn Hưng, (2009). Nghiên cứu, điều chế titan dioxit kích thước nanomet từ tinh quặng inmenit Hà Tĩnh bằng axit sunfutic. *Tạp chí Hóa học*, 145-149.

[14] L. G. Devi and R. Kavitha, (2014). Enhanced photocatalytic activity of sulfur doped TiO_2 for the decomposition of phenol: a new insight into the bulk and surface modification (in E). *Materials Chemistry and Physics,* **143(3)**, 1300-1308.

[15] Rengifo-Herrera J. A., Mielczarski E., Mielczarski J., Castillo N. C., Kiwi J., and Pulgarin C., (2008). Escherichia coli inactivation by N, S co-doped commercial TiO2 powders under UV and visible light, (in E). *Applied Catalysis B: Environmental,* **84(3-4)**, 448-456.

[16] Jia T., F. Fu, D. Yu, J. Cao, and G. Sun, (2018). Facile synthesis and characterization of N-doped TiO_2/C nanocomposites with enhanced visible-light photocatalytic performance. *Applied Surface Science* **430**, 438-447.

[17] Greczynski G. and L. Hultman, (2020). X-ray photoelectron spectroscopy: towards reliable binding energy referencing. *Progress in Materials Science,* **107**, 100591.

[18] Kochuveedu S. T. *et al.*, (2011). Visible-light active nanohybrid TiO2/carbon photocatalysts with programmed morphology by direct carbonization of block copolymer templates. *Green Chemistry*, **13(12)**, 3397-3405.

[19] Shen K., X. Xue, X. Wang, X. Hu, H. Tian, and W. Zheng, (2017). One-step synthesis of band-tunable N, S co-doped commercial TiO_2/graphene quantum dots composites with enhanced photocatalytic activity. *RSC Advances*, **7(38)**, 23319-23327.

[20] Yu J. C., Ho W., Yu J., Yip H., Wong P. K., and Zhao J., (2005). Efficient visible-light-induced photocatalytic disinfection on sulfur-doped nanocrystalline titania. *Environmental science & technology,* **39(4)**, 1175-1179.

[21] Liu S. and Chen X., (2008). A visible light response TiO_2 photocatalyst realized by cationic S-doping and its application for phenol degradation," (in E). *Journal of Hazardous Materials,* **152(1)**, 48-55.

[22] Kang S., R. Mauchauffé, Y. S. You, and S. Y. Moon, (2018). Insights into the role of plasma in atmospheric pressure chemical vapor deposition of titanium dioxide thin films. *Scientific reports,* **8(1)**, 1-13.

[23] Park Y., W. Kim, H. Park, T. Tachikawa, T. Majima, and W. Choi (2009). Carbon-doped TiO_2 photocatalyst synthesized without using an external carbon precursor and the visible light activity. *Applied Catalysis B: Environmental,* **91(1-2)**, 355-361.

[24] Y. Wang, Y. Huang, W. Ho, L. Zhang, Z. Zou, and S. Lee, (2009). Biomolecule-controlled hydrothermal synthesis of C-N-S-tridoped TiO_2 nanocrystalline photocatalysts for NO removal under simulated solar light irradiation. *J. Hazard. Mater.*, 1**69(1-3)**, 77–87.

[25] Y. Huynh and N. Le, (2015). N-TiO_2 synthesized by reflux method in H_2O_2-urea solution: point of zero charge, adsorption propertives, and photocatalytic activities under visible light. *Science and Technology Development Journal,* **18(1)**, 81-91.